Journal of Southeast University (English Edition) Vol. 39, No. 4, pp. 416 - 425 Dec. 2023 ISSN 1003—7985

Preparation and analysis on graphene oxide-silver/graphene oxide/chitosan composite antibacterial dressing

Liu Haohuai He Zhizhou Wang Yufei Peng Lingxi

(School of Chemistry and Chemical Engineering, Guangzhou University, Guangzhou 510006, China)

Abstract: Graphene oxide was prepared by the modified Hummers method and ultrasonic peeling method. Ammoniacal silver solution and green glucose were added to the fresh achieved graphene oxide suspension to prepare graphene oxide-silver (GO-Ag) nanoparticles. The prepared GO-Ag nanoparticles were incorporated into chitosan and graphene oxide to prepare graphene oxide-silver/graphene oxide/chitosan (GO-Ag/GO/CS) composites. The structure and properties of GO-Ag/GO/CS composite were investigated by SEM, XRD, TG, tensile test and antibacterial test. SEM and XRD analysis indicate that GO-Ag is successfully compounded with graphene oxide and chitosan mixture. Tensile test show that the incorporation of graphene oxide into chitosan matrix can effectively improve the tensile strength of GO-Ag/GO/CS composite, especially the wet-state tensile strength. Thermogravimetric analysis indicate that the incorporation of graphene oxide has a slight effect on the thermal stability of CS. The results of antibacterial test illustrate that when the addition of GO-Ag particles is 5.0 mg, the bacteriostatic rate of GO-Ag/GO/CS against *S. aureus* and *E. coli* can reach 98.40% and 100%, respectively, showing excellent bacteriostatic effect.

Key words: graphene oxide-silver; chitosan; nanoparticle composite; antibacterial

DOI: 10.3969/j.issn.1003 - 7985.2023.04.011

The skin acts as a natural barrier of the human body preventing microbial invasion and playing an important role in maintaining the stability of the internal environment. If the skin is damaged, a large number of denatured and necrotic tissues as well as effusion of plasma-like components will seep out of the wounds, and pathogens such as *S. aureus* and *E. coli* are prone to multiply in wounds, causing wound infection and making it difficult to be healed. In some cases for patients with extensive skin trauma, pathogenic bacteria may enter the body causing serious infections like sepsis, meningitis or bacteremia, with life-threatening potential[1]. Therefore, to construct an ideal antibacterial wound dressing without drug-resistance and reduce serious infection caused by wound pathogens, has become a crucial research direction in the field of trauma treatment.

In order to prevent wound infection, much effort has been made to add antibacterial substances to wound dressings. Due to the wide application of various antibacterial drugs, the bacterium has developed new drug-resistant bacterial strains. The noble metal antibacterial agent such as silver nanoparticle is widely favored due to their lack of drug resistance[1-3]. However, there are still some problems needed to be solved when transferring silver nanoparticles to biological media, for silver nanoparticles tend to aggregate to minimize their surface energy in the process of preparation, leading to reduce the antibacterial efficiency[4]. In this regard, a practical method is to anchor them on support matrix, which can not only improve the stability, but also enhance their antibacterial properties[5]. Such a suitable material is graphene oxide (GO), which is usually a single or multi-layer graphite oxide exfoliated from graphite[6]. Graphene oxide with a transverse size of micrometer can be used as an effective template for anchoring silver nanoparticles, avoiding the agglomeration of silver nanoparticles during the synthesis process[7-8]. In recent years, many studies have demonstrated that graphene oxide-silver (GO-Ag) composites have better antibacterial properties than silver nanoparticles[7,9-10]. Therefore, GO-Ag can be used as an outstanding nano-antibacterial agent to improve the antibacterial property of medical dressings.

Among various medical dressing materials, chitosan based biological dressings have been one of the most widely studied and applied. Chitosan is a natural cationic polysaccharide generated by the deacetylation of chitin which is abundant in nature[11], and mostly comes from bacteria, fungi and the shells of shrimp and crab[12]. Chitosan has great advantages in air permeability which can activate macrophages and promote wound healing[13]. Chitosan also has good biocompatibility and biodegradability, antibacterial, anti-inflammatory, anti-acid, anti-ulcer, anticoagulant properties[13-14]. Moreover, chitosan can be used to make various forms of wound dressings such as membranes, coatings, hydrogels, fibers, powders, and nanoparticles. It has broad application pros-

Received 2023-05-24, **Revised** 2023-09-09.

Biography: Liu Haohuai (1981—), female, doctor, senior experimentalist, huaihuai99@163.com.

Foundation item: Science and Technology Projects of Guangzhou (No. 202102010481).

Citation: Liu Haohuai, He Zhizhou, Wang Yufei, et al. Preparation and analysis on graphene oxide-silver/graphene oxide/chitosan composite antibacterial dressing[J]. Journal of Southeast University (English Edition), 2023, 39(4): 416 - 425. DOI: 10.3969/j.issn.1003 - 7985.2023.04.011.

pects in medical dressings and artificial skin[15].

Taking into account the properties of the above discussed materials, the present study is combining the advantages of GO-Ag particles and chitosan to prepare graphene oxide-silver/graphene oxide/chitosan (GO-Ag/GO/CS) composite dressing. The physicochemical and antibacterial properties of GO-Ag/GO/CS composites were investigated, with the expectation that GO-Ag/GO/CS composite may have a good prospect to be used as antibacterial medical dressing for skin tissue engineering.

1 Materials and Methods

1.1 Materials

Graphite powder (99.9%), chitosan (degree of deacetylation is 80% to 95%) and silver nitrate($AgNO_3$) were purchased from China National Pharmaceutical Group Co., Ltd. (Sinopharm); Potassium permanganate ($KMnO_4$), sodium nitrate ($NaNO_3$), sulfuric acid (95%), hydrogen peroxide (30%), hydrochloric acid (37%), barium chloride ($BaCl_2$), anhydrous dimethyl sulfoxide (DMSO), aqueous ammonia and glucose were obtained from local manufacturers. All reagents used in this research were analytical grade.

1.2 Preparation of graphene oxide

Graphene oxide was prepared by modified Hummers method[16]. Firstly, 5 g graphite powder was mixed with 115 mL sulfuric acid uniformly in ice water bath (no more than 5 ℃), then 2.5 g sodium nitrate and 15 g $KMnO_4$ were added gradually to the mixture. After stirring for 2 h, the ice water bath was replaced by warm water bath with the temperature maintained at 35 ℃ for 30 min. In the next step, 230 mL of distilled water was added into the beaker under rapid stirring, and the reaction temperature was maintained at 90 ℃, the stirring time was kept for 30 min. After diluting the reaction solution to 600 mL with distilled water, a certain amount of hydrogen peroxide (3% to 5%) was added until the suspension was golden yellow. Then, the solution was washed with 5% hydrochloric acid and distilled water repeatedly and centrifuged until the graphite oxide aqueous dispersion was neutral and no white precipitate was formed by $BaCl_2$ detection. Finally, the prepared graphite oxide was exfoliated by ultrasonic vibration at the frequency of 60 kHz for 1 h to obtain graphene oxide suspension.

1.3 Preparation of graphene oxide-silver nanoparticles

Silver ammonia solution was prepared as follows: 2.04 g silver nitrate was dissolved in suitable distilled water to prepare 100 mL solution (0.12 mol/L). Then, 10 mL silver nitrate solution (0.12 mol/L) was taken into a test tube, 2.5% ammonia water was added drop by drop with shaking the test tube until the initial precipitate just disappeared completely, and then silver ammonia solution was obtained. In the next step, graphene oxide suspension containing 204 mg of graphene oxide was put into a beaker, and distilled water was added to dilute it to 100 mL. Then, the fresh silver ammonia solution was added into graphene oxide suspension and stirring for 30 min at 50 ℃. And next, 1 g glucose (dissolved in 50 mL distilled water) was added into the mixture and the mixture was heated to 90 ℃ with stirring for 1 h. After cooling, it was centrifuged, washed and filtered with ethanol and distilled water for several times to obtain graphene oxide-silver nanoparticles, and then the obtained graphene oxide-silver nanoparticles were freeze-dried for later use.

1.4 Preparation of graphene oxide-silver/graphene oxide/chitosan composites

A certain amount of graphene oxide suspension (the mass ratio of graphene oxide to chitosan is 0∶100, 2∶100, 4∶100, 6∶100 and 8∶100, respectively) was added into a beaker, distilled water was added to dilute it to 100 mL, 2 mL glacial acetic acid was added to the beaker before 3 g chitosan was added into it, and then the mixture was stirred at high speed for 0.5 h. Afterwards, 3.0 mg GO-Ag was added into the mixture, stirred at high speed for 0.5 h until a homogenous solution was obtained, and next, the mixture was left at room temperature for 2 h without being disturbed before being casted onto a plate mould at room temperature for 2 h. Subsequently, the mould was put into an oven at 40 ℃ for 24 h. Finally, the film was fully washed with deionized water and dried at room temperature to obtain graphene oxide-silver/graphene oxide/chitosan composite (GO-Ag/GO/CS). The obtained composite film was labeled as GO-Ag3/GO/CS and the GO-Ag/GO/CS composite films with different GO-Ag content (4.0, 5.0 and 6.0 mg) were prepared using the same procedure and labeled as GO-Ag4/GO/CS, GO-Ag5/GO/CS, GO-Ag6/GO/CS, respectively.

1.5 Characterization

UV-visible spectra were recorded in the range between 200 and 800 nm using ultraviolet spectrograph (UV-2550, Japan). The graphene oxide suspension and GO-Ag suspension were diluted 10 times to record the UV-visible spectra. The morphology of the prepared samples was investigate by scanning electron microscope (JEOL 6700, Japan) and the energy-dispersive spectrum (EDS) was performed by the EDS system (Bruker 60, Germany) to analyze the element presence of the samples. XRD measurements were performed using an X-ray diffractor (PW3040/60, Netherlands) with Cu Kα radiation (λ = 0.154 nm) operating at 40 kV and 40 mA. Tensile tests were carried out on dumbbell-shaped samples cut from the center of the films using a punch. The tensile strengths of GO-Ag/GO/CS composite films were measured by an

electronic universal testing instrument (UT4304, China) at a cross-head speed of 50 mm/min according to GB/T 1040.3—2006. The thermal stability of GO-Ag/GO/CS composites was carried out on a thermogravimetric analyzer (TGA4000, USA). The measurements were carried out in a nitrogen atmosphere from 30 to 550 ℃ at a heating rate 10 ℃/min.

The swelling behaviors of CS and GO-Ag/GO/CS composite films were evaluated at room temperature using a conventional gravimetric analysis method. Dry CS and GO-Ag/GO/CS samples in a diameter of 20 mm were weighted and immersed in distilled water for predetermined time intervals. At each time point, the wet weights of the samples were recorded after removing excessive surface water with filter paper. The swelling degree was calculated as

$$S = \frac{100(W_{wet} - W_{dry})}{W_{dry}} \quad (1)$$

where W_{dry} and W_{wet} are the weights of dry samples and swollen samples. All data points were the means of five different measurements.

1.6 Cytotoxicity test

1.6.1 Cell culture

In vitro cytotoxicity of GO/CS and GO-Ag/GO/CS composites with different GO-Ag contents (0, 3.0, 4.0, 5.0 and 6.0 mg) were evaluated using MTT assay by culturing with mouse fibroblasts NIH-3T3 cells. Each slice specimen, 15.0 mm in diameter, was washed 5 times with deionized water under ultrasonic vibration, following sterilization by steam for 20 min at 121 ℃ and 136 kPa pressure. The specimens were then placed in 24-well cell culture plates (Corning, USA) with 1 mL of fresh medium in each well for 1 h, and NIH-3T3 cells cultured in media for 3 d were seeded on the top of pre-wetted specimens (2×10^4 cells/specimen) with 1 mL culture medium into each well. The specimens were left undisturbed in a humidified incubator at 37 ℃ with 95% air and 5% CO_2 for 1, 3, 5 and 7 d. The media was changed every two days. The morphologies of NIH-3T3 cells cultured with GO-Ag/GO/CS composites were observed by optical microscope.

1.6.2 MTT assay

After culturing for 24, 48, and 72 h, the supernatant medium was removed, and the samples were transferred to new wells of 24-well plates. Then, 40 μL/well of MTT solution and additional 1 mL culture medium was added into each sample, the cells were incubated at 37 ℃ for 4 h to allow the formation of formazan crystal. After the incubation, supernatant medium was removed, 450 μL dimethyl sulfoxide (DMSO) was added to each well to dissolve the formazan crystals with shaking. After shaking for 5 min, the solution of each sample was removed out for assay in a 96-well plate. The optical density (OD) was read on Wallac victor 1420 multilabel counter (PerkinElmer, USA) using a test wavelength of 490 nm. The results from four individual experiments were averaged. The relative growth rate R of cells was obtained by dividing the OD value of the experimental group by the OD value of the blank group. Cytotoxicity was evaluated based on the relative growth rate of cells, when $R_s \geqslant 100\%$, the cytotoxicity level is evaluated as level 0. When R_s is within the range of 75% to 99%, the cytotoxicity level is evaluated as level Ⅰ. Both level 0 and level Ⅰ are non-cytotoxic levels, which satisfy the safety standards of biomaterials.

1.7 Antibacterial activity test

Each disc specimen with 6.0 mm in diameter was put into glass tube filled with 2 mL bacterial suspension (1×10^6 CFU/mL) and incubated in a shaking incubator at 37 ℃ for 24 h. After incubation, 200 μL of bacterial suspension was taken out from the culture medium and diluted by appropriate times, afterwards, 100 μL of bacteria suspension was collected and smeared on agar plate uniformly, then the agar plate was turned over and incubated at 37 ℃ for 24 h. Following incubation, the numbers of bacterial colonies on the agar plate were counted, the results from three individual experiments were averaged. The bacteria suspension without samples treated with the same procedure was used as the control group, and the bacteriostatic rate R was calculated as

$$R = \frac{N_c - N_s}{N_c} \times 100\% \quad (2)$$

where N_c is the number of bacterial colonies in the control group, CFU/mL; N_s is the number of bacterial colonies in the experimental group, CFU/mL.

1.8 Statistical analysis

All the data were given as means ± standard deviations. Statistical difference was analyzed using one-way analysis of variance (ANOVA) on GraphPad InStat 3.05 (GraphPad Software, USA). A value of $p < 0.05$ was considered to be statistically significant.

2 Results and Discussion

2.1 UV spectra

Fig. 1 shows the UV-visible spectra of the dispersions of GO and GO-Ag. It can be seen from GO spectra that GO exhibits two characteristic peaks which are similar to those already reported in Ref. [2]. The absorption peak at 230 nm is assigned to the characteristic absorption peak of carbon skeleton on GO, and the shoulder absorption peak at 300 nm is the characteristic absorption peak of C═O group on GO. After adding silver nitrate and Ag particles

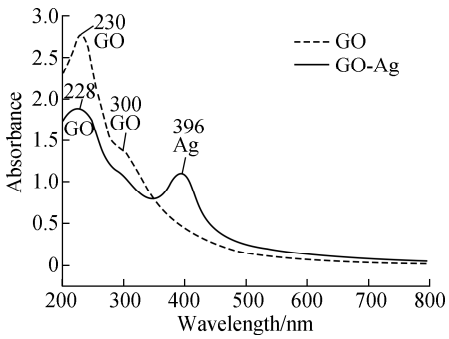

Fig. 1 UV spectra

generated, the shoulder absorption peak of GO dispersion at 300 nm disappeared, and a new peak at 396 nm occurred, which can be assigned to the surface plasmon resonance (SPR) absorption band of Ag nanoparticles, suggesting the formation of Ag nanoparticles. In addition, the characteristic absorption peak (228 nm) of carbon skeleton on GO still exists, which indicates that the formation of Ag nanoparticles does not change the structure of GO matrix.

2.2 Morphology analysis

The morphology of GO obtained by TEM was shown in Fig. 2(a). It was observed that GO with a layered structure has many silk-like wrinkles on the surface, which is the characteristic morphology of GO. Fig. 2(b) showed the morphology of the synthesized GO-Ag composite. It

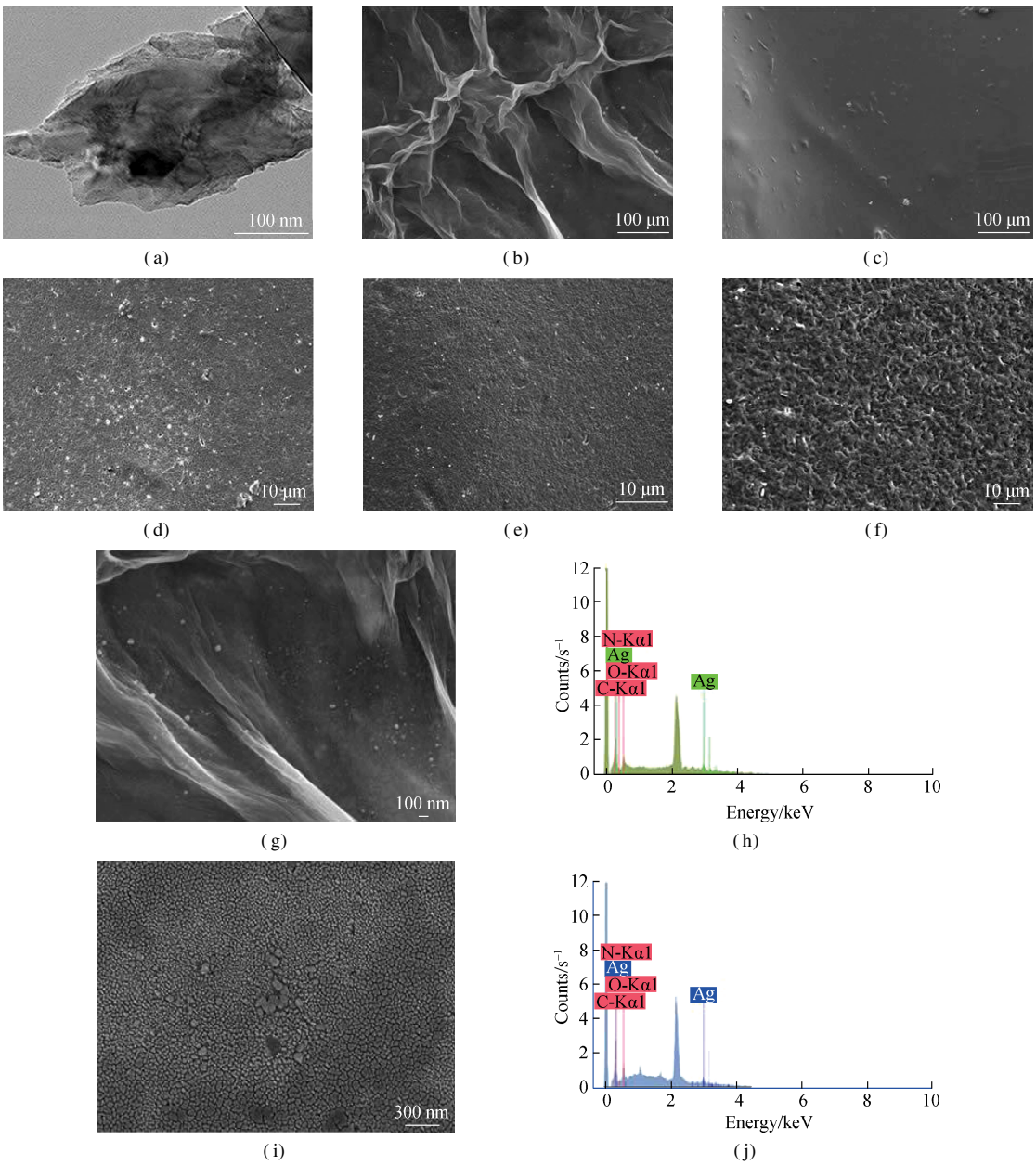

Fig. 2 Morphology images. (a) TEM of GO; (b) SEM of GO-Ag (20 000 ×); (c) CS membrane at low magnification (200 ×); (d) CS membrane at high magnification (1 000 ×); (e) GO-Ag/GO/CS membrane at low magnification (200 ×); (f) GO-Ag/GO/CS membrane at high magnification (1 000 ×); (g) GO-Ag at high magnification (30 000 ×); (h) EDS spectra of GO-Ag; (i) GO-Ag/GO/CS membrane at high magnification (100 000 ×); (j) EDS spectra of GO-Ag/GO/CS

can be seen that the wrinkles still appear on the graphene sheets, and many spherical silver nanoparticles with a size of 20-30 nm are distributed on the graphene oxide surface without agglomeration. Because there are many functional groups on the base and edge of graphene oxide, which can act as nucleation sites of silver nanoparticles, so silver ions are anchored stably onto graphene oxide surface in the process of gradual reduction[5,8], which can avoid the agglomeration of the formed silver nanoparticles[7] and limit the free release of silver nanoparticles from the matrix[17]. The EDS spectrum of GO-Ag was shown in Fig. 2(h), it revealed the existence of carbon, nitrogen, oxygen and Ag elements in the GO-Ag composite. Carbon, nitrogen and oxygen came from GO, while Ag was attributed to the presence of Ag nanoparticles. The experimental results of Ref. [5] showed that when the mass ratio of GO to silver nitrate is 1∶1, the prepared silver particles are distributed uniformly and densely, without agglomeration phenomenon. Tang et al. [18] and Dat et al. [5] showed that when the mass ratio of GO to silver nitrate is 1∶1, the GO-Ag nanoparticles have the strongest antibacterial ability to *S. aureus* and *E. coli*, so the mass ratio of graphene oxide to silver nitrate used to prepare GO-Ag is also 1∶1 in this experiment.

Figs. 2(c) to (f) show the SEM photographs of pure CS and GO-Ag/GO/CS membranes. It can be seen that the pure CS membrane (see Figs. 2(c) and (d)) shows a small porous and smooth surface phase, while the GO-Ag/GO/CS composite membrane (see Figs. 2(e) and (f)) exhibits a small irregular pores and rough surface phase. The pores and roughness on the membrane surface are essential for cells adhesion and crawl. At higher magnification (see Fig. 2(i)) of GO-Ag/GO/CS membrane, the Ag nanoparticles are observed in the CS matrix, and the EDS spectra shown in Fig. 2(j) revealed the existence of carbon, nitrogen, oxygen and Ag elements in the GO-Ag/GO/CS composite. Carbon, nitrogen and oxygen came from GO and CS, while Ag element was derived from Ag nanoparticles in the composite.

2.3 XRD patterns

Fig. 3 shows the XRD patterns of GO, GO-Ag, CS, GO-Ag/GO/CS composite and GO/CS composite. In the GO pattern, the obvious diffraction peak at $2\theta = 11.7°$ appears, while in GO-Ag pattern, the diffraction peak at $2\theta = 11.7°$ disappears, which indicates that graphene oxide is partially reduced to graphene by the reaction of reducing agent glucose. In GO-Ag pattern, the characteristic peaks at the diffraction angles of 38.0°, 44.2°, 64.3° and 77.2° are attributed to the planes (111), (200), (220) and (311) of crystal structure of Ag nanoparticles, which indicates that silver ions are reduced simultaneously by glucose, and GO-Ag nanoparticles are prepared. It can be seen from CS pattern that CS shows two characteristic peaks at $2\theta = 10.3°$ and $2\theta = 20.3°$, while the characteristic peaks in GO/CS pattern at $2\theta = 10.3°$ and $2\theta = 20.3°$ are weakened, which may be attributed to the interface interaction between graphene oxide and chitosan reducing the crystallization degree of CS. In the GO-Ag/GO/CS pattern, the characteristic peaks of CS matrix at $2\theta = 10.3°$ and $2\theta = 20.3°$ still exist, and the characteristic peaks of Ag (111), (200), (220) and (311) appear at the same time, which indicates that GO-Ag is successfully compounded with graphene oxide and chitosan, and the structure of GO-Ag does not change after being compounded with chitosan and graphene oxide.

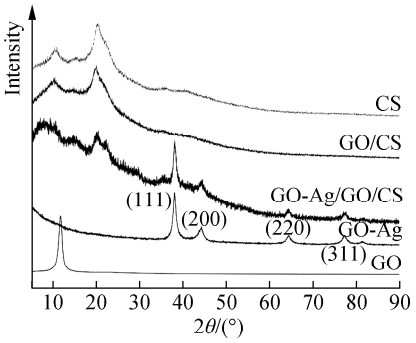

Fig. 3 XRD patterns

2.4 Tensile properties

In this experiment, the effect of GO content on the tensile strength of GO-Ag/GO/CS composites were investigated by keeping GO-Ag content unchanged (4.0 mg) and changing GO content from 0 to 8%. The GO-Ag/GO/CS composite with GO contents of 2%, 4%, 6% and 8% were defined as GO-Ag/GO2/CS, GO-Ag/GO4/CS, GO-Ag/GO6/CS and GO-Ag/GO8/CS. Fig. 4 shows the dry-state and wet-state tensile strength of GO-Ag/GO/CS composites with GO content increasing. It can be seen from Fig. 4 that in the range of GO content of this study, with the increase of GO content, the dry-state and wet-state tensile strengths of composites have been greatly improved compared with the dry-state and wet-state tensile strength of chitosan matrix. On the one hand, it can be attributed to the nano-scale effect of GO; on the other hand, it can be attributed to the strong hydrogen bonding between the hydroxyl, carboxyl groups on the surface of GO and the hydroxyl groups on the surface of chitosan, which enhances the interfacial bonding strength of GO-Ag/GO/CS. When the content of GO is lower, the molecular chains of the composites are pulled apart under the action of external force, and the GO sheets play a reinforcing role in dispersing stress, transferring and dissipating energy. Therefore, with the increase of GO content, the dry-state and wet-state tensile strength of the composites increase synchronously. When the content of GO is 4%, the dry-state and wet-state ten-

sile strength of the composites synchronously arrive at the maximum(127.6 and 15.4 MPa, respectively). Compared with the dry-state tensile strength (74.3 MPa) and wet-state tensile strength (4.9 MPa) of chitosan matrix, the dry-state and wet-state tensile strengths of the composites are increased by 71.7% and 214.3%, respectively. It can be seen that the addition of GO can effectively improve the tensile strength of chitosan matrix, especially the wet-state tensile strength. It is more necessary to improve the wet-state tensile strength of chitosan composite for chitosan is a poor water resistant material. However, when the content of GO is too high, agglomeration of GO will weaken the nano-scale effect and can be the centre of stress convergence when under tensile stress, so the tensile strength of the composite decreases with the increase of GO. But the decline is relatively slow, when the content of GO is 8%, there is no significant difference ($p > 0.05$) in dry-state tensile strength compared to the composite with a content of 6% GO.

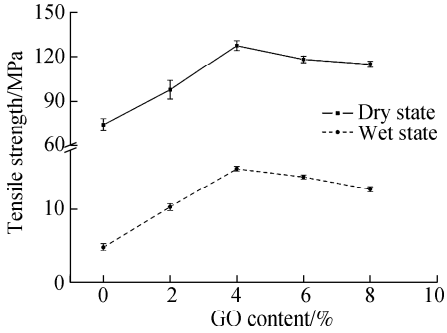

Fig. 4 Effects of GO content on tensile strength of GO-Ag/GO/CS composites

2.5 Thermogravimetric analysis

The thermal degradation of CS and GO-Ag/GO/CS composites with various GO contents were studied by thermo-gravimetric analysis and the results were shown in Fig. 5. As for the pure GO, the initial weight loss in first decomposition stage from 50 to 100 ℃ is attributed to the elimination of free water from samples. The main decomposition region for pure GO is from 130 to 250 ℃, in which the oxygenated functionalities presented on GO layer have decomposed. It can be seen from the TG curve that the thermal decomposition trend of GO-Ag/GO/CS composite is similar to that of pure chitosan, which is divided into two stages: the first decomposition stage is 60 to 130 ℃ in which free water is removed from the samples, and the second decomposition stage is 200 to 340 ℃ in which the chitosan matrix begins to decompose as well as the decomposition of oxygenated functionalities on GO layer. From each TG and DTG curves, the following data are taken into account: 1) T_{20}, the temperature at which 20% of weight loss occurs has been taken as the temperature deviating from the thermogravimetric curve platform by the degradation of matrix; 2) T_{50}, the temperature at which 50% weight loss occurs; 3) T_{max}, the temperature is defined as the highest maximum of the DTG curve. The parameters determined from thermogravimetric analysis are presented in Table 1. It can be seen that the thermal stability of the GO-Ag/GO/CS composites has been improved slightly compared to the pure CS. This slight increase indicates the positive effect of GO on the thermal stability of GO-Ag/GO/CS composites, which has also been confirmed by Khan et al[19]. They ascribed the improvement of thermal stability to the strong interfacial interaction between GO and chitosan matrix. However, the thermal stability of those composites does not increase continuously with increasing loading levels of GO. When the content of GO is higher than 4%, the thermal stability of those composites presents a slightly decrease which may be attributed to the agglomeration of GO will weaken the interfacial interaction between GO and chitosan matrix. The high-temperature resistance of GO-Ag/GO/CS composite recommends them for high-temperature sterilization processes, which is the most common method for

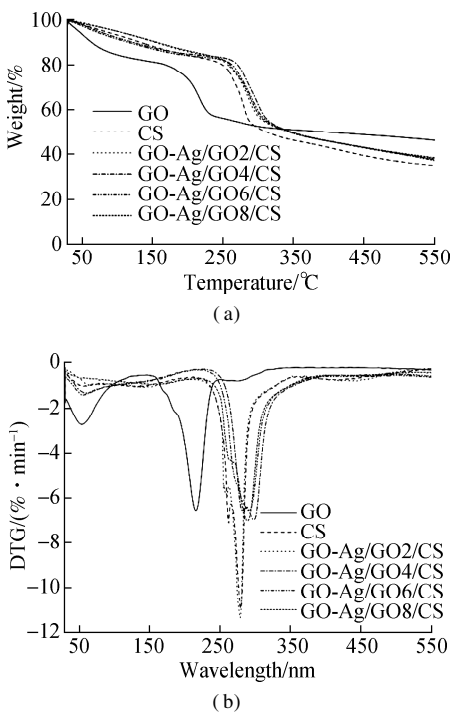

Fig. 5 TG and DTG curves for pure GO and GO-Ag/GO/CS composite films with various GO loadings. (a) TG curves; (b) DTG curves

Table 1 Thermal degradation parameters of CS and GO-Ag/GO/CS composites ℃

Specimens	$T_{20\%}$	$T_{50\%}$	T_{max}
GO	165.45	371.16	215.20
CS	247.22	307.67	279.57
GO-Ag/GO2/CS	248.73	311.28	279.56
GO-Ag/GO4/CS	269.57	341.61	298.02
GO-Ag/GO6/CS	261.36	341.46	289.74
GO-Ag/GO8/CS	258.73	338.61	288.96

hospital sterilization due to their low cost and minimal environmental impact.

2.6 Swelling measurements

Studying swelling behavior is important because it can predict how much the film will swell when in contact with biological fluids, and prevent large expansion of the film as well as avoid possible compression of the wounds. The swelling degree of CS and GO-Ag/GO/CS composite films were shown in Fig. 6. The water uptake process of samples in distilled water is a dynamic equilibrium process, the swelling degree is initially higher and then gradually increasing slowly, after 1 h, the water uptake performance reaches equilibrium. It was found that the presence of GO in GO-Ag/GO/CS composite tends to reduce the swelling behavior. This is mainly because GO is less hydrophilic than CS. CS has a large number of polar groups such as amino and hydroxyl groups, which are easy to interact with water molecules in the form of hydrogen bonds or network water retention, allowing the molecular chain gradually expand to absorb water. When the GO content is low, it has less hindrance and restriction on the mobility of CS chains, at this time, GO itself also absorbs a certain amount of water. Therefore, the water uptake performance of GO-Ag/GO/CS composite is not significantly different from that of pure CS ($p > 0.05$). However, as the GO content continues to increase, the strong interaction between GO and CS matrix tends to hinder and limit the binding of amino and hydroxyl groups with water molecules. At this time, there are more cross-linking points, resulting in smaller micropores in the network structure, which is not conducive to the penetration of water. Therefore, the blocking effect of GO dominates, causing the swelling degree of GO-Ag/GO/CS composite begin to decrease, which may be beneficial for GO-Ag/GO/CS composites to maintain their integrity for a longer period of time in comparison with pure CS.

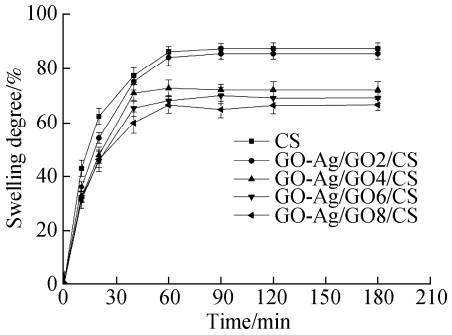

Fig. 6 Swelling degree of CS and GO-Ag/GO/CS composites over time

2.7 Cytotoxicity test

According to above-mentioned analysis results, the tensile strength of GO-Ag/GO/CS composites reaches the maximum when the GO content is 4%, so in this experiment we kept GO content at 4%, and changed GO-Ag content from 0 to 6.0 mg to investigate the effect of GO-Ag addition on the cytotoxicity and antibacterial activity of GO-Ag/GO/CS composites.

Fig. 7 shows the cell morphologies of mouse fibroblasts NIH-3T3 cells cultured with the GO-Ag/GO/CS composites for 3 and 5 d. It can be seen from Fig. 7 that the number of cells increases with the extension of culture time. After 3 d of culture, the cells of all groups attached to the wall and sprawled out with a fusiform and polygon shape. Cell growth statuses of GO/CS, GO-Ag3/GO/CS, GO-Ag4/GO/CS and GO-Ag5/GO/CS are similar, without cell senescence and abnormal division phenomenon, but there were some dead cells appeared around the GO-Ag6/GO/CS group. After 5 d of culture, the cells of all groups had proliferated to a level of dense distribution, and the cells grew vigorously, aggregated with each other to form a confluent layer. However, the number of dead cells in GO-Ag6/GO/CS group increased slightly. The co-culture of cells and materials experiments indicate that

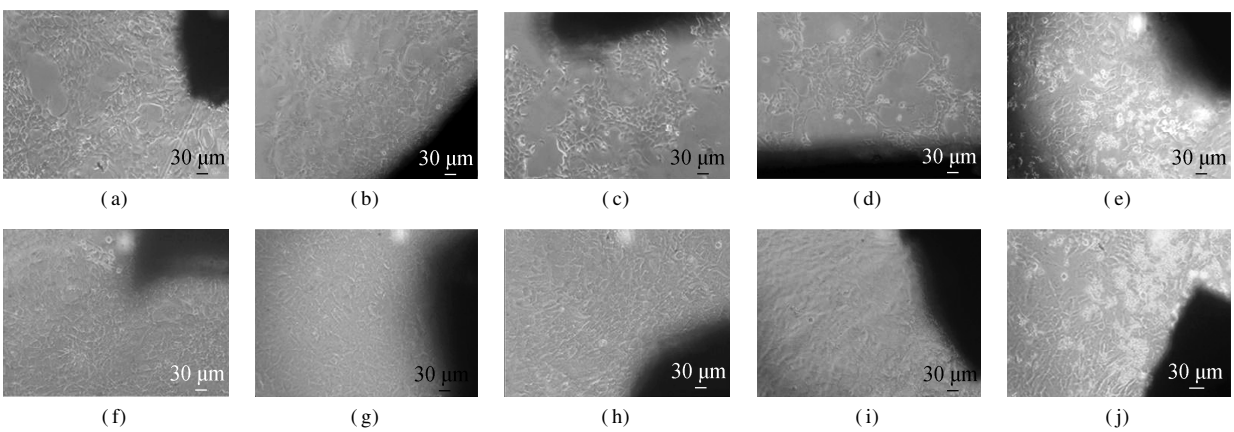

Fig. 7 Light microscopic images of NIH-3T3 cells cultured with GO-Ag/GO/CS composites. (a) GO/CS (3 d); (b) GO-Ag3/GO/CS (3 d); (c) GO-Ag4/GO/CS (3 d); (d) GO-Ag5/GO/CS (3 d); (e) GO-Ag6/GO/CS (3 d); (f) GO/CS (5 d); (g) GO-Ag3/GO/CS (5 d); (h) GO-Ag4/GO/CS (5 d); (i) GO-Ag5/GO/CS (5 d); (j) GO-Ag6/GO/CS (5 d)

GO/CS, GO-Ag3/GO/CS, GO-Ag4/GO/CS and GO-Ag5/GO/CS composite had no cytotoxicity, only GO-Ag6/GO/CS had a little cytotoxicity.

MTT assay was used to compare the relative growth rate G and cytotoxicity of mouse fibroblasts NIH-3T3 on different composites. The cells inoculated on the blank culture plate were used as the control. Cell viability and relative growth rate in each group evaluated after 24, 48 and 72 h incubation were shown in Fig. 8 and Table 2. As shown in Fig. 8, GO/CS, GO-Ag3/GO/CS, GO-Ag4/GO/CS and GO-Ag5/GO/CS are found to have no significant difference in cell proliferation ($p > 0.05$) compared with the cells on blank control. Only GO-Ag6/GO/CS group has significant difference in cell proliferation ($p < 0.05$) compared with the cells on the blank control group. It can be seen from Table 3, when the addition of GO-Ag is 3.0-5.0 mg, the relative growth rates of cells at 24, 48 and 72 h are all greater than 90%, while, when the addition of GO-Ag is 6.0 mg, the relative growth rates at 24, 48 and 72 h were 84%, 81% and 78%, respectively, although it showed an obvious decline, the corresponding cytotoxicity levels are still all level Ⅰ, which satisfy the safety standards of biomaterials and can be used for further experimental study.

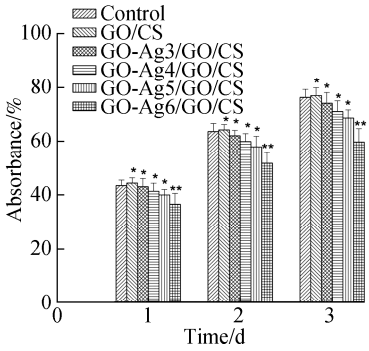

Fig. 8 MTT assay of NIH-3T3 proliferation on different GO-Ag/GO/CS composite films at different culture time ($^{*}p > 0.05$, $^{**}p < 0.05$)

Table 2 Relative growth rate and cytotoxicity levels of cells with different culture time in different GO-Ag/GO/CS composite groups

Specimens	24 h		48 h		72 h	
	R/%	Cytotoxicity level	*R*/%	Cytotoxicity level	*R*/%	Cytotoxicity level
Control	100	0	100	0	100	0
GO/CS	102	0	101	0	101	0
GO-Ag/GO3/CS	99	Ⅰ	98	Ⅰ	97	Ⅰ
GO-Ag/GO4/CS	95	Ⅰ	94	Ⅰ	93	Ⅰ
GO-Ag/GO5/CS	92	Ⅰ	91	Ⅰ	90	Ⅰ
GO-Ag/GO6/CS	84	Ⅰ	81	Ⅰ	78	Ⅰ

Table 3 Bacteriostatic rate of different GO-Ag/GO/CS composite groups against *S. aureus* and *E. coli* %

Specimens	*S. aureus*	*E. coli*
Blank control	0	0
GO-Ag3/GO/CS	$62.05 \pm 0.04^{**}$	$76.11 \pm 0.05^{**}$
GO-Ag4/GO/CS	$88.60 \pm 0.03^{**}$	$94.54 \pm 0.03^{**}$
GO-Ag5/GO/CS	$98.40 \pm 0.01^{**}$	100^{**}
GO-Ag6/GO/CS	$99.74 \pm 0.01^{**}$	100

Note: $^{**}p < 0.05$.

2.8 Antibacterial activity

It is widely believed that bacteria can colonize on both biological and abiotic surfaces. In the early stages of chronic wound formation, Gram-positive bacteria, especially *S. aureus*, accounts for the majority. Then Gram-negative bacteria, such as *E. coli* and *Pseudomonas*, appear and tend to invade the deeper skin, causing serious tissue injury[20-21]. So, in this experiment, Gram-positive bacteria *S. aureus* and Gram-negative bacteria *E. coli* were chosen as the test bacteria to evaluate the antibacterial effect of GO-Ag/GO/CS composite dressing. The photography representations of antibacterial effects of GO-Ag/GO/CS composite against *S. aureus* and *E. coli* are shown in Fig. 9 and the bacteriostatic rate of GO-Ag/GO/CS composite are shown in Table 3. It can be seen from Fig. 9 and Table 3 that the bacteriostatic rate against *S. aureus* of GO-Ag3/GO/CS is only 62.05%, while that of GO-Ag4/GO/CS is 88.60%, when the addition of GO-Ag particles is 5.0 mg, its bacteriostatic rate against *S. aureus* can reach 98.40%. When the addition of GO-Ag particles increases to 6.0 mg, the bacteriostatic rate against *S. aureus* can reach 99.74%. As can be shown, GO-Ag/GO/CS composites have higher antibacterial activity against *E. coli* than against *S. aureus*, when the addition of GO-Ag particles is 3.0 mg, the bacteriostatic rate against *E. coli* is 76.11%, when the addition of GO-Ag particles increase to 4.0, 5.0 and 6.0 mg, the bacteriostatic rate against *E. coli* reaches 94.54%, 100% and 100%, respectively. It can be concluded that the bacteriostatic rate of GO-Ag/GO/CS composite against *S. aureus* and *E. coli* both increase with the increase of GO-Ag addition, and the antibacterial effect against *E. coli* bacteria is more active than *S. aureus* bacteria. On the one hand, positively charged Ag^{+} ions can be firmly attached to the cell membrane surface of negatively charged *E. coli* by electrostatic attraction, resulting in reproductive dysfunction and rapid death of *E. coli* bacteria[22]. On the other hand, Gram-positive bacteria piles up many peptidoglycan in the cell walls[23], making it more difficult for Ag^{+} ions to destroy the bacterial cell membrane of *S. aureus*

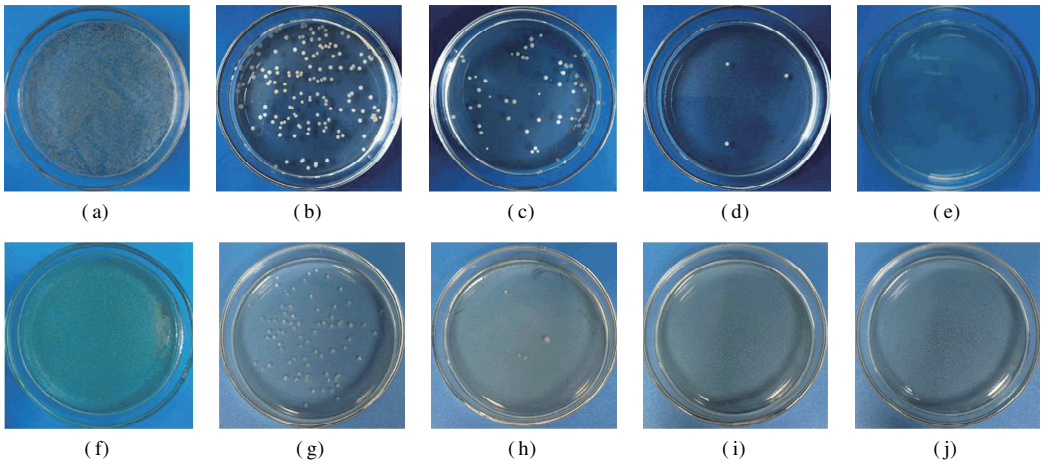

Fig. 9 Photographic representations of antibacterial activity of GO-Ag/GO/CS composites against *S. aureus* and *E. coli*. (a) Control against *S. aureus*; (b) GO-Ag3/GO/CS against *S. aureus*; (c) GO-Ag4/GO/CS against *S. aureus*; (d) GO-Ag5/GO/CS against *S. aureus*; (e) GO-Ag6/GO/CS against *S. aureus*; (f) Control against *E. coli*; (g) GO-Ag3/GO/CS against *E. coli*; (h) GO-Ag4/GO/CS against *E. coli*; (i) GO-Ag5/GO/CS against *E. coli*; (j) GO-Ag6/GO/CS against *E. coli*

compared to *E. coli*. Therefore, the antibacterial effect of GO-Ag/GO/CS composite on *E. coli* was more obvious than that of *S. aureus*.

From the results of cytotoxicity test and antibacterial test, it can be seen that the cytotoxicity levels of all experimental groups of composite dressing are level Ⅰ. When the addition of GO-Ag particles is 5.0 or 6.0 mg, the bacteriostatic rate against *S. aureus* and *E. coli* are higher than 98%, showing excellent bacteriostatic effect, but considering the relative growth rate of cells and bacteriostatic effect, the appropriate addition of GO-Ag particles is 5.0 mg in GO-Ag/GO/CS composite. Combined with the results of tensile test and thermal degradation test, it can be concluded that GO-Ag/GO/CS composite containing 4% GO and 5 mg GO-Ag is recommended for future experimental studies.

3 Conclusions

1) GO-Ag nanoparticles were successfully prepared by loading silver nanoparticles on graphene oxide with glucose as a green reducing agent. The achieved GO-Ag nanoparticles were successfully incorporated into graphene oxide and chitosan mixture to prepare GO-Ag/GO/CS composites.

2) The results were very promising in terms of improving the tensile strength of chitosan-based dressing by the addition of GO. Thermogravimetric analysis indicates that the addition of GO has a slight effect on the thermal stability of CS.

3) The antibacterial test showed that the added GO-Ag played an important role in improving the antibacterial activity of the CS-based dressing. When the addition of GO-Ag particles is 5.0 mg, the bacteriostatic rate against *S. aureus* and *E. coli* of GO-Ag/GO/CS composite are higher than 98%, showing excellent bacteriostatic effect, which is recommended for future experimental study.

References

[1] Bal-Ozturk A, Ozkahraman B, Ozbas Z, et al. Advancements and future directions in the antibacterial wound dressings—a review[J]. *Journal of Biomedical Materials Research Part B: Applied Biomaterials*, 2021, **109**(5): 703－716. DOI: 10.1002/jbm.b.34736.

[2] Marta B, Potara M, Iliut M, et al. Designing chitosan-silver nanoparticles-graphene oxide nanohybrids with enhanced antibacterial activity against Staphylococcus aureus [J]. *Colloids and Surfaces A: Physicochemical and Engineering Aspects*, 2015, **487**: 113－120. DOI: 10.1016/j.colsurfa.2015.09.046

[3] Huang J, Cao M F, Ma Y X, et al. Wastewater treatment performance and microbial community structure in the constructed wetland under double-pressure of low temperature and Ag NPs exposure[J]. *Journal of Southeast University (English Edition)*, 2022, **38**(3): 291－299. DOI: 10.3969/j.issn.1003-7985.2022.03.011.

[4] Huong N T, Dat N M, Thinh D B, et al. Optimization of the antibacterial activity of silver nanoparticles-decorated graphene oxide nanocomposites [J]. *Synthetic Metals*, 2020, **268**: 116492. DOI: 10.1016/j.synthmet.2020.116492.

[5] Dat N M, Thinh D B, Huong L M, et al. Facile synthesis and antibacterial activity of silver nanoparticles-modified graphene oxide hybrid material: The assessment, utilization, and anti-virus potentiality[J]. *Materials Today Chemistry*, 2022, **23**: 100738. DOI: 10.1016/j.mtchem.2021.100738.

[6] Guo L P, Wang H, Chen B, et al. Dispersion of graphene in silane coupling agent aqueous solutions[J]. *Journal of Southeast University (English Edition)*, 2020, **36**(1): 67－72. DOI: 10.3969/j.issn.1003-7985.2020.01.009.

[7] Khorrami S, Abdollahi Z, Eshaghi G, et al. An improved method for fabrication of Ag-GO nanocomposite with controlled anti-cancer and anti-bacterial behavior; a comparative study[J]. *Scientific Reports*, 2019, **9**: 9167. DOI: 10.1038/s41598-019-45332-7.

[8] Islami M, Zarrabi A, Tada S, et al. Controlled quercetin

release from high-capacity-loading hyperbranched polyglycerol-functionalized graphene oxide [J]. *International Journal of Nanomedicine*, 2018, **13**: 6059 - 6071. DOI: 10.2147/IJN.S178374.

[9] Zhu Z J, Su M, Ma L, et al. Preparation of graphene oxide-silver nanoparticle nanohybrids with highly antibacterial capability[J]. *Talanta*, 2013, **117**: 449 - 455. DOI: 10.1016/j.talanta.2013.09.017.

[10] Jaworski S, Wierzbicki M, Sawosz E, et al. Graphene oxide-based nanocomposites decorated with silver nanoparticles as an antibacterial agent[J]. *Nanoscale Research Letters*, 2018, **13**: 116. DOI: 10.1186/s11671-018-2533-2.

[11] Tan Q Y, Kan Y J, Zhao G T, et al. Pressure-induced strong adhesion between chitosan nanofilms[J]. *Journal of Southeast University* (*English Edition*), 2015, **31**(1): 113 - 117. DOI: 10.3969/j.issn.1003-7985.2015.01.019.

[12] Li Z, Zhang Y, Shen Y M, et al. The study on the relationship between the molecular structures of chitosan derivatives and their hydrate inhibition performance [J]. *Journal of Molecular Liquids*, 2022, **364**: 120007. DOI: 10.1016/j.molliq.2022.120007

[13] Seidi F, Yazdi M K, Jouyandeh M, et al. Chitosan-based blends for biomedical applications[J]. *International Journal of Biological Macromolecules*, 2021, **183**: 1818 - 1850. DOI: 10.1016/j.ijbiomac.2021.05.003.

[14] Tang C, Zhao B, Zhu J J, et al. Preparation and characterization of chitosan/sodium cellulose sulfate/silver nanoparticles composite films for wound dressing[J]. *Materials Today Communications*, 2022, **33**: 104192. DOI: 10.1016/j.mtcomm.2022.104192.

[15] Peng W, Li D, Dai K L, et al. Recent progress of collagen, chitosan, alginate and other hydrogels in skin repair and wound dressing applications[J]. *International Journal of Biological Macromolecules*, 2022, **208**: 400 - 408. DOI: 10.1016/j.ijbiomac.2022.03.002.

[16] Marcano D C, Kosynkin D V, Berlin J M, et al. Improved synthesis of graphene oxide[J]. *ACS Nano*, 2010, **4**(8): 4806 - 4814. DOI: 10.1021/nn1006368.

[17] Li P H, Zou X Y, Wang X D, et al. A preliminary study of the interactions between microplastics and citrate-coated silver nanoparticles in aquatic environments[J]. *Journal of Hazardous Materials*, 2020, **385**: 121601. DOI: 10.1016/j.jhazmat.2019.121601.

[18] Tang J, Chen Q, Xu L G, et al. Graphene oxide-silver nanocomposite as a highly effective antibacterial agent with species-specific mechanisms[J]. *ACS Applied Materials & Interfaces*, 2013, **5**(9): 3867 - 3874. DOI: 10.1021/am4005495.

[19] Khan Y H, Islam A, Sarwar A, et al. Novel green nanocomposites films fabricated by indigenously synthesized graphene oxide and chitosan[J]. *Carbohydrate Polymers*, 2016, **146**: 131 - 138. DOI: 10.1016/j.carbpol.2016.03.031.

[20] Liang Y Q, Liang Y P, Zhang H L, et al. Antibacterial biomaterials for skin wound dressing[J]. *Asian Journal of Pharmaceutical Sciences*, 2022, **17**(3): 353 - 384. DOI: 10.1016/j.ajps.2022.01.001.

[21] Simoes D, Miguel S P, Ribeiro M P, et al. Recent advances on antimicrobial wound dressing: A review[J]. *European Journal of Pharmaceutics and Biopharmaceutics*, 2018, **127**: 130 - 141. DOI: 10.1016/j.ejpb.2018.02.022.

[22] Bi C L, Zhang C H, Ma F Q, et al. Development of 3D porous Ag^+ decorated PCN-222 @ graphene oxide-chitosan foam adsorbent with antibacterial property for recovering U (VI) from seawater[J]. *Separation and Purification Technology*, 2022, **281**: 119900. DOI: 10.1016/j.seppur.2021.119900.

[23] Kasinathan K, Marimuthu K, Murugesan B, et al. Synthesis of biocompatible chitosan functionalized Ag decorated biocomposite for effective antibacterial and anticancer activity[J]. *International Journal of Biological Macromolecules*, 2021, **178**: 270 - 282. DOI: 10.1016/j.ijbiomac.2021.02.127.

氧化石墨烯-银/氧化石墨烯/壳聚糖复合抗菌敷料的制备与分析

刘浩怀　何芝洲　王玉飞　彭凌西

(广州大学化学化工学院, 广州 510006)

摘要:采用改进的 Hummer 法和超声波剥离法制备氧化石墨烯,并在新制的氧化石墨烯悬液中加入银氨溶液和绿色葡萄糖,得到氧化石墨烯-银(GO-Ag)纳米粒子,将其加入壳聚糖和氧化石墨烯中,获得氧化石墨烯-银/氧化石墨烯/壳聚糖(GO-Ag/GO/CS)复合材料. 采用 SEM、XRD、TG、拉伸实验和抗菌实验等方法分析了 GO-Ag/GO/CS 复合材料的结构和性能. SEM 和 XRD 分析结果表明,GO-Ag 与氧化石墨烯和壳聚糖基体成功复合. 拉伸实验结果表明,GO 的加入能够显著提高 GO-Ag/GO/CS 复合材料的拉伸强度,尤其是湿态拉伸强度. 热失重分析结果表明,GO 的引入对壳聚糖基体的热稳定性影响较小. 抗菌实验结果表明,当 GO-Ag 的添加量为 5.0 mg 时,GO-Ag/GO/CS 对金黄色葡萄球菌和大肠杆菌的抑菌率分别可达 98.04% 和 100%,展现出优异的抑菌效果.

关键词:氧化石墨烯-银;壳聚糖;纳米复合物;抗菌

中图分类号:R318